Desulfurization Properties of Activated Carbon Fibers

Wei Liu, PhD[1], Sabit Adanur, PhD[2]

[1]Intertek Consumer Goods NA, Arlington Heights, IL UNITED STATES

[2]Auburn University, Auburn, AL UNITED STATES

Correspondence to:
Sabit Adanur email: adanusa@auburn.edu

ABSTRACT
Activated carbon fibers (ACFs) are one of the most promising adsorbents due to their outstanding properties, such as more exposed adsorption surface, narrower pore size distribution, fast adsorption rate and flexibility, in comparison with granular activated carbon and activated carbon powder. In this work, ACFs manufactured from various raw materials were studied and their pore structures and sulfur dioxide removal performance under dry and humid conditions were investigated. From the ACFs studied in this paper, larger surface area was found correspond to higher total pore volume and larger DA micropore diameter. In dry air, breakthrough capacity of ACFs with sulfur dioxide was found to be proportionately dependent on micropore ratio and pore size distribution. Although powdered activated carbon (PAC) showed higher breakthrough capacity, its adsorption rate was slower than ACFs due to the difference of the pore structure. The presence of water vapor in the air stream greatly increased SO_2 adsorption capacities of ACFs but affected their utilization differently.

Keywords: Activated carbon fibers, sulfur dioxide

INTRODUCTION
Porous adsorbents have been widely used in purification and filtration systems for complete removal of sulfur dioxide (SO_2) through adsorption either with physisorption or chemisorption. One of the most popular adsorbents is activated carbons; because of their broad capability in filtration to remove particulate materials, heavy metals, organic materials, and other air toxics [1]. Activated carbons can be classified into three categories according to their shape: granular activated carbon (GAC), powdered activated carbon (PAC), and extruded activated carbon (EAC). Activated carbon fiber (ACF) is a relatively new adsorbent used for filtration and purification techniques. Compared with GAC and PAC, ACFs have outstanding characteristics as desulfurization agents [2]. The features of pores in ACFs are different from GAC. Most of the pores in ACFs are micropores with the presence of some mesopores and macropores. Due to the small fiber diameters, pores can directly reach the center of fibers and therefore the diffusion path of adsorbate to reach the adsorption sites is short. The pore schematics of typical ACF and GAC structures are shown in *Figure 1*.

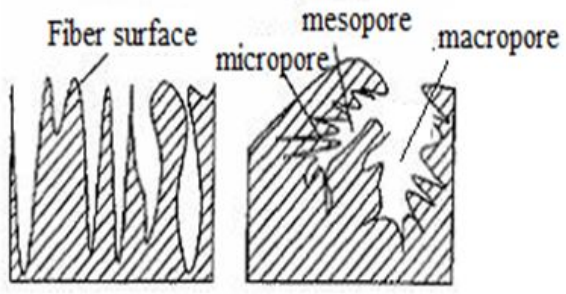

FIGURE 1. Schematic of pore structures of ACF and GAC [3].

The more open structure may contribute to a reduced possibility of blocked pores. GAC and PAC have plenty of micropores and mesopores which adsorbates usually reach after passing macropores. The blockage of macropores would limit the access of adsorbates to smaller pores where adsorption would occur. ACF generally has a narrower pore size distribution and a higher surface area. Small fiber diameters also result in a larger contact surface area between adsorbents and adsorbates and thus even contact can be achieved.

All of these characteristics of ACF may explain the faster adsorption rate and higher adsorption capacity in desulfurization process [4]. ACFs are able to remove not only high concentration contaminants but also low concentration contaminants [2]. ACFs have also been found to have lower pressure drop compared to GAC. ACF has a lower volume density and lower filtration resistance, which is about 1/3 of GAC. Therefore, unlike GAC, ACFs are able to filter liquids with a higher viscosity and less penalty of

energy consumption. ACFs offer fabrication flexibility which GAC does not have, and thus they can be easily made into filter media or devices. ACFs can be made in various forms such as fabrics, nonwovens, paper and composites, which make them suitable for handling in special devices [4-7]. Considering the outstanding properties of materials in nanoscale, activated carbon fibers were also made in nanoscale and their porous structure and other structural parameters were studied [8-12]. Zhao et al. pointed to some merits of ACFs in specific applications. In water purification systems, ACFs have the advantage of being less likely to produce ash, have a lower pressure drop and a higher water flow rate. In air purification systems, ACFs show faster adsorption and desorption rates. In ammonia, toluene, sulfur dioxide and nitrogen dioxide cleaning systems, ACFs showed high removal efficiency and adsorption capacity [2].

EXPERIMENTAL

Materials

Five types of activated carbon fibers are studied in this paper, namely ACF10, ACF15, ACF20, CR and SY. They are classified based on the precursors. ACF10, ACF15 and ACF20 were made from Kynol™ novoloid fibers by American Kynol, Inc. CR, purchased from Carbon Resources, Inc., is rayon-based ACF in the form of felt. SY is rayon-based ACF felt provided by Senyou Carbon Fiber Co., Ltd (China). For the purpose of comparison, powdered activated carbon (PAC) is studied as well. Activated carbon powder (60~140 mesh) is manufactured from coconut shell by PICA, Inc.

Pore Structure

Pore characteristics of activated carbon, such as Brunauer-Emmett-Teller (BET) surface area, average pore size and pore volume, were analyzed based on isotherms obtained on Autosorb-1 (Quantachrome® Instruments) using nitrogen as adsorbate at 77 K.

Sulfur Dioxide Adsorption Testing

Dynamic SO_2 adsorption characteristics of bare ACFs as well as PAC were analyzed based on breakthrough curves which were obtained through adsorption tests performed in a fixed tubular column reactor made of glass. The experimental test bench was designed based on the ASTM D6646-01 Standard Test Method for Determination of the Accelerated Hydrogen Sulfide Breakthrough Capacity of Granular and Pelletized Activated Carbon and is shown in *Figure 2*.

The challenge gas containing SO_2 was fed into the glass reactor. The SO_2 concentration was monitored and recorded on a SO_2 single gas detector (BW Gasalert Extrem). Breakthrough times and breakthrough curves were obtained during each test and the corresponding SO_2 capacities were calculated.

RESULTS AND DISCUSSION

Pore Structure of Activated Carbon Fibers

According to the International Union of Pure and Applied Chemistry (IUPAC), pores are classified into three categories, namely micropore, mesopore, and macropore with pore sizes less than 2 nm, between 2 and 50 nm, and larger than 50 nm, respectively. Surface area, total pore volume, average pore diameter and micropore diameter (calculated according to the Dubinin-Astakhov equation) of ACFs and PAC are summarized in *Table I*.

TABLE I Pore properties of the materials used.

	ACF10	ACF15	ACF20	CR	SY	PAC
BET surface area (m^2/g)	784.2	1370	2247	1763	806	913
Total pore volume (cc/g)	0.51	0.88	1.462	1.09	0.515	0.6
Average pore diameter (Å)	24.28	25.79	26.03	24.88	25.5	26.82
DA micropore width (Å)	11.97	15	17.69	16	14	14.2

On the Autosorb-1, surface area was estimated based on BET equation by assuming that a monolayer of nitrogen molecules covers the adsorbent surfaces. The total pore volume was derived from the amount of vapor adsorbed at a relative pressure close to unity, by assuming that the pores are filled with liquid adsorbates.

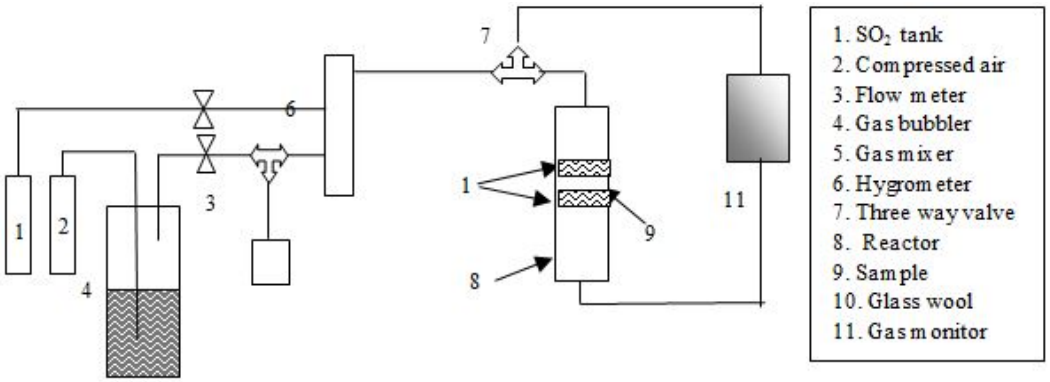

FIGURE 2. Schematic of the SO_2 adsorption test bench.

The average pore diameter was evaluated from the total pore volume. To characterize micropores, the Dubinin-Astakhov (DA) equation is more appropriate for strongly activated carbon [13-15], which is used in this research:

$$W = W_0 exp\left[-\left(\frac{-RTln(\frac{P}{P_0})}{E}\right)^n\right] \quad (1)$$

where, W is the weight adsorbed at P/P_0 and T, P is the pressure of adsorbate, Po is the saturated vapor pressure of adsorbate, T is the adsorption temperature, W_0 is the total weight adsorbed, E is the characteristic energy and n is a non-integer value (typically between 1 and 3) [15]. Characteristic energy is the measure of the mean value of adsorption potential which is a measure of the affinity of the surface for the adsorbate molecules for microporous adsorbents. The values of component n and E were found to be related to pore size distribution. High value of n and low value of E represent narrow pore size distribution [13].

ACF10, ACF15 and ACF20 were made from the same precursors but exhibiting different pore properties as shown in *Table I*, which is due to the variation of activation conditions. ACF20 with a higher surface area, more pore volume and larger average pore size was activated at a higher temperature. Regardless of the precursors, the total pore volume shows linear relation with the surface area: higher surface area corresponds to higher total pore volume, as shown in *Figure 3*. Since the majority of pores is micropores as shown in *Table II*, a similar trend is shown between surface area and micropore volume. Although the average pore diameter fluctuates in a narrower range of 24.28 and 26.82 as shown in *Table I*, regardless of precursors and activation conditions, the DA micropore diameter is dependent on surface area: the higher the surface area, the larger the micropore diameter.

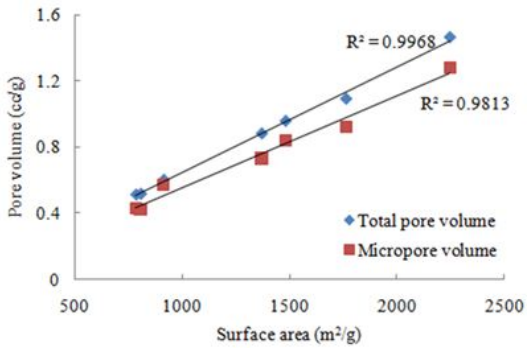

FIGURE 3. Relation between surface area and total pore volume.

TABLE II. Pore volume distributions of activated carbon fibers and powdered active carbon.

DA pore analysis	ACF 10	ACF 15	ACF 20	CR	SY	PAC
Micropore (cc/g)	0.376	0.611	0.966	0.665	0.385	0.427
Mesopore (cc/g)	0.051	0.12	0.314	0.262	0.039	0.138
Macropore ($\times 10^{-4}$ cc/g)	1.92	2.81	12.7	13.9	0.323	18.5
Total pore volume (cc/g)	0.427	0.731	1.28	0.928	0.424	0.567
Micropore percentage (%)	88	83.55	75	71.63	90.73	75.33
Mesopore percentage (%)	11.98	16.41	24.53	28.22	9.26	24.35
Macropore percentage (%)	0.045	0.038	0.099	0.015	0.008	0.033
E (kJ/mol)	8.59	6.6	5.67	5.36	7.41	7.11
n	1.9	2.1	1.9	1.8	2.5	1.4

Pore size distribution (PSD) of ACFs and PAC based on the DA equation is illustrated in *Table II* and *Figure 4*. For the ACFs made from novoloid fibers, the values of n are close to each other; ACF10 and ACF20 have the highest and lowest characteristic energy, respectively, indicating a narrower PSD of ACF10.

Since the ACF20 was more activated than ACF10, separated micropores in ACF20 hay have expanded and thus connected with the neighboring micropores resulting in the formation of macropores. However, the value of n and E cannot generally represent the shape of pore size distribution for all ACFs and PAC studied in this work. The number of adsorption sites of ACFs and PAC, which is considered to contribute to the adsorption of adsorbate over adsorbents, are summarized in *Table III.*

TABLE III. Number of adsorption sites.

Samples	ACF10	ACF15	ACF20	CR	SY	PAC
Number of adsorption sites ($\times 10^{20}$)	2.99	5.22	8.56	6.72	3.07	3.48

Sulfur Dioxide Adsorption Properties of Activated Carbon Fibers

Sulfur Dioxide Adsorption over Bare Activated Carbon Fibers in Dry Air

ACFs were subjected to 20 ppm SO_2 carried by air at a face velocity of 33cm/s at room temperature. When water vapor is absent in the gas stream, SO_2 is expected to be adsorbed onto free sites on fiber

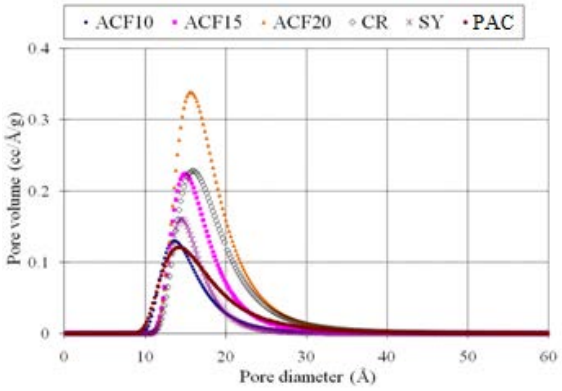

FIGURE 4 Pore size distributions of ACFs and PAC.

surfaces where they are oxidized to sulfur trioxide. The resulting breakthrough time (BT), breakthrough capacity (BC), saturation capacity (SC) and utilization of ACFs and PAC are summarized in *Table IV*. The utilization of samples refers to the ratio of breakthrough time to saturation time.

TABLE IV. Sulfur dioxide capacities of bare activated carbon fibers in dry air*.

	ACF 10	ACF 15	ACF 20	CR	SY	PAC
BT (min)	4.67	3.57	1.4	7.67	14.75	19
BC (mg SO_2/g sample)	1.72	1.32	0.45	2.85	5.05	7.07
SC (mg SO_2/g sample)	4.26	1.98	1.99	5.52	10.68	16.39
Utilization (%)	14.15	16.23	5.83	10.22	22.69	19.79

*Sample weight: 0.5 g, initial SO_2 concentration: 20 ppm, face velocity: 35 cm/s at 20ºC.

Samples are classified according to the precursors, namely novoloid-based ACFs and rayon-based ACFs. For novoloid-based ACFs, ACF10 with 88% micropores exhibited the highest breakthrough capacity of 1.72 mg SO_2/g adsorbent while ACF20 with the least micropore ratio gave the lowest breakthrough capacity of 0.45 mg SO_2/g adsorbent. In the rayon-based ACF group, SY with 90.73% micropores is more capable in desulfurization than CR, whose micropore ratio is 71.63%. In other words, SO_2 breakthrough capacity of ACFs in dry condition is proportionately dependent on the micropore ratio or on pore size distribution for each group. Thus the higher the micropore ratio, the higher the breakthrough capacity. More micropores in adsorbents indicate a lower ratio of mesopores and macropores through which adsorbates have to pass before reaching adsorption sites in micropores where adsorption usually occurs. Blockage is more likely to happen if there are more macropores in adsorbents. Furthermore, SO_2 capacity for each group of ACFs was inversely proportional to micropore pore size, pore volume and surface area, which can be explained by the concept proposed by Marsh et al., where adsorbents with smaller pores adsorb contaminants better at lower concentrations due to a higher overlap in potential between the pore and walls [14-16].

Breakthrough profiles of the activated carbon fibers are shown in *Figure 5* when water vapor is absent in the carrier gas. ACF10, ACF15, ACF20 and CR became saturated by SO_2 quickly after breakthrough in comparison with SY and PAC which have lower slopes in breakthrough curves. SY exhibited the highest utilization of 22.69% (*Table IV).* Although PAC has a longer breakthrough time and thus higher breakthrough capacity, the breakthrough curve of PAC has lower slope which reflects the slower adsorption rate, probably due to harder access of adsorbates to free sites in pores. Micropores in ACFs

allow adsorbate to reach the fiber center directly while, in PAC, adsorbates have to pass through macropores in order to reach micropores where adsorption usually happens [17].

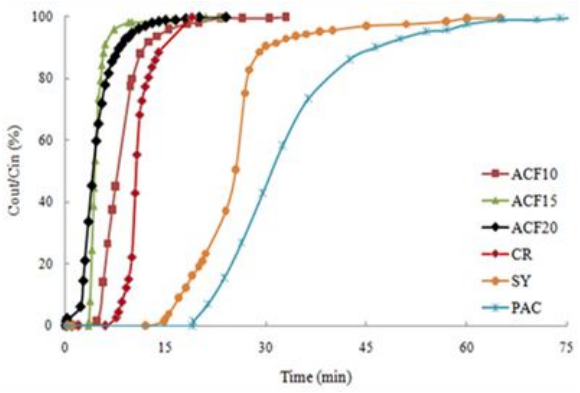

FIGURE 5. Breakthrough profiles of activated carbon fibers in dry air (C_{in}:20 ppm, velocity: 33 cm/s, sample weight: 0.5 g) (C_{in}: 20 ppm, velocity: 33 cm/s, sample weight: 0.5 g).

The diameter of PAC was measured to be 290 μm, which is much larger than 12 μm of ACFs. Although ACF20 and PAC have very similar micropore ratios, micropores in PAC may be imbedded in the middle and therefore it may be hard for adsorbates to reach.

With the absence of water vapor in the carrier gas, SY exhibited the highest breakthrough capacity with the longest period before breakthrough among all ACFs. The spent SY felts were regenerated both in air (110°C for 2 hour) and nitrogen (600°C for 1 hour). Air-regenerated SY at 110°C gave a breakthrough capacity of 1.98 mg SO_2/g adsorbent, which is 39.21% of the original capacity, while the nitrogen-regenerated SY shows a breakthrough capacity of 6.5 mg SO_2/g adsorbent, which is 50% of the initial capacity, in dry air. The saturation capacity of nitrogen-regenerated SY is 4.93 mg SO2/g adsorbent, i.e., 46.16% of the fresh SY.

Sulfur Dioxide Adsorption over Bare Activated Carbon Fibers in Humidified Air

As shown in *Table V* and *Figure 6*, the presence of water vapor in the main gas stream greatly increased SO_2 capacities of ACFs while their utilizations were affected by water vapor differently. Utilizations of ACF10, ACF15, ACF20 and CR were improved since their breakthrough times were greatly increased, while those of SY and PAC were reduced because they needed longer time to achieve saturation as shown in breakthrough curves in *Figure 6.* For activated carbons fibers, the outlet SO_2 concentration first increased quickly after breakthrough; then the rate of increase slowed down, causing longer time to achieve saturation. The increased capacity is attributed to the water vapor which eventually promoted the continuous removal of SO_2 through a series of procedures which was proposed by Mochida et al., [18]. The oxidized SO_2, sulfur trioxide, is hydrated by water producing sulfuric acid which is attached to the fiber surfaces occupying the adsorption sites. If extra water vapor is available, adsorbed sulfuric acid is eluted to aqueous form from fiber surface releasing occupied adsorption sites for further SO_2 adsorption, facilitating the continuous removal of SO_2.

TABLE V. Sulfur dioxide capacities of bare activated carbon fibers with the presence of water vapor*.

	ACF 10	ACF 15	ACF 20	CR	SY	PAC
BT (min)	25	18.5	14.67	24	19.75	24
BC (mg SO_2/g sample)	7.92	6.84	5.46	8.73	6.99	8.86
80% SC (mg SO_2/g sample)	13.89	20.1	37.32	32.23	44.94	74.81
Utilization (%)	21	25.26	10.55	16.78	7.68	5.8

*Sample weight: 0.5 g, initial SO_2 concentration: 20 ppm, face velocity: 35 cm/s, relative humidity: 100%, temperature: 20ºC.

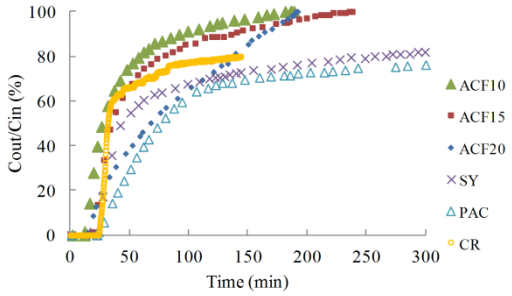

FIGURE 6. Breakthrough profiles of ACFs with the presence of water vapor in the carrier gas (initial SO_2 concentration: 20 ppm, face velocity: 33 cm/s, sample weight: 0.5 g).

When water vapor was present in the carrier gas, the breakthrough capacity of novoloid-based ACFs is still proportionally related to the micropore ratio of ACFs, which is the same trend as those with the absence of water vapor. However, their saturation capacities increased with the surface area and pore volume. In comparison with fibers, PAC has a higher breakthrough capacity if water vapor is absent in the carrier gas. If the air is humidified before mixing with SO_2, the breakthrough capacity of CR becomes close to PAC but saturation capacity of PAC is higher.

CONCLUSION

Among the ACFs studied in this paper, regardless of precursors, total pore volume and DA micropore diameter were found to be related to the surface area: higher surface area corresponds to a higher total pore volume and larger DA micropore diameter.

In dry air, the breakthrough capacity of ACFs on SO_2 was proportionately dependent on micropore ratio and pore size distribution for each ACF group. Although PAC showed higher breakthrough capacity, its adsorption rate was slower than ACFs due to the difference of the pore structure.

The presence of water vapor in the air stream greatly increased SO_2 adsorption capacities of ACFs but affected their utilization differently.

ACKNOWLEDGEMENT

The authors wish to thank the colleagues at the Center for Microfibrous Materials Manufacturing for their help.

REFERENCES

[1] Debarr, J. A., Lizzio, A. A., and Daley, M. A., Adsorption of SO_2 on bituminous coal char and activated carbon fiber, *Energy & Fuels*, 11, 2, 1997, 267-271.

[2] Zhao, L., Huang, X., Gu, Q. et al., The performance comparison of granular activated carbon filter and fiber filter of activated carbon, *Contamination Control & Air-conditioning Technology*, Issue 2, 2004, 17-20.

[3] Wey, M. Y., Fu, C. H., Tseng, H. H., et al., Catalytic oxidization of SO_2 from incineration flue gas over bimetallic Cu-Ce catalysts supported on pre-oxidized activated carbon, *Fuel*, 82, 18, 2003, 2285-2290.

[4] Wang, J. Y., Zhao, F. Y., Hu, Y. Q., et al., Modification of activated carbon fiber by loading metals and their performance on SO_2 removal, *Chinese Journal of Chemical Engineering*, 14 (4), 2006, 478-485.

[5] Edens, R. L., Gadsby, E. D., Lindsay, J. D., et al., Kimberly-Clark Worldwide, Inc. , Flexible activated carbon substrates, U.S. Patent Application Publication No.: US 2004/0121688 A1, Jun. 24, 2004.

[6] Hsieh, S.-J., Clothing material structure of fiber cloth containing PAN series activated carbon, U.S. Patent Application Publication No: US 2004/0092188 A1, May 13, 2004.

[7] Giglia, R. and Battistelli, E., American Cyanamid Company Non-woven activated carbon fabric, patent 4904343, USA, 1990.

[8] Liu, W., and Adanur, S., Properties of electrospun polyacrylonitrile membranes and chemicall-actived carbon nanofibers, *Textile Research Journal*, 80, 2, 2010, 124-134.

[9] Liu, C., Lai, K., Liu, W., et al., Preparation of carbon nanofibres through electrospinning and thermal treatment, *Polymer International*, 58, 12, 2009, 1341-1349.

[10] Yacoob, C., Liu, W. and Adanur, S. "Properties and flammability of electrospun PVA and PVA/Laponite membranes", *Journal of Industrial Textiles*, 40, 1, 2010, 33-48.

[11] Yee, S., Liu, W. and Adanur, S. "Properties of electrospun PVA/nanoclay composite", *Journal of the Textile Institute*, Submitted.

[12] Liu, C., Sun, R., Lai, K., Branscomb, D., and Liu, W. "Electrospinning well-aligned fiber arrays through a modified collector", *Journal of Xi'an Polytechnic University*, 23, 2, 2009, 114-118.

[13] Burevski, D., The application of the Dubinin-Astakhov equation to the characterization of microporous carbons, *Colloid and Polymer Science*, 260, 6, 1982, 623-627.

[14] Marsh, H. and Rand, B., The characterization of microporous carbon by means of the dubinin-radushkevich equation, *Journal of Colloid and Interface Science*, 33, 1970, 101-116.

[15] Autosorb-1 AS1 Win Version 1.51 operating manual, Boynton Beach, Florida USA, 2005.

[16] Daley, M. A., Mangun, C. L., Debarr, J. A., et al., Adsorption of SO_2 onto oxidized and heat-treated activated carbon fibers (ACFS), *Carbon*, 35 (3), 1997, 411-417.

[17] Liu, W., Activated carbon fiber filter media for proton exchange membrane fuel cell, PhD dissertation, Polymer and Fiber Engineering, Auburn University, May 2010, Page 20-21.

[18] Mochida, I., Korai, Y., Shirahama, M., et al., Removal of Sox and NO_x over actived carbon fibers, *Carbon*, 38, 2, 2000, 227-239.

AUTHORS' ADDRESSES

Wei Liu, PhD
Intertek Consumer Goods NA
545 E Algonquin Road, Suite C
Arlington Heights, IL 60005
UNITED STATES

Sabit Adanur, PhD
Auburn University
115 Textile Building
Auburn, AL 36849
UNITED STATES